frontiers | Frontiers in Materials

TYPE Original Research
PUBLISHED 17 September 2025
DOI 10.3389/fmats.2025.1657286

OPEN ACCESS

EDITED BY
Pietro Calandra,
National Research Council (CNR), Italy

REVIEWED BY
Mohammad M. Karimi,
Tarbiat Modares University, Iran
Zhenxiang Xie,
Sun Yat-sen University, China
Cesare Oliviero Rossi,
University of Calabria, Italy

*CORRESPONDENCE
Fanlong Tang,
tangfanlong@jit.edu.cn

RECEIVED 01 July 2025
ACCEPTED 28 August 2025
PUBLISHED 17 September 2025

CITATION
Fan X, Shan G, Fan J and Tang F (2025) Performances of SBS and Nano-TiO_2 composite modified asphalt and mixture after repetitive aging and regeneration.
Front. Mater. 12:1657286.
doi: 10.3389/fmats.2025.1657286

Performances of SBS and Nano-TiO_2 composite modified asphalt and mixture after repetitive aging and regeneration

Xuefeng Fan[1], Gang Shan[2], Jianwei Fan[2,3] and Fanlong Tang[3]*

[1]Jiangshan Highway and Harbor Transportation Management Center, Quzhou, China, [2]School of Transportation, Southeast University, Nanjing, China, [3]College of Network and Communication Engineering, Jinling Institute of Technology, Nanjing, China

The long-term durability of SBS–nano TiO_2 composite modified asphalt and mixtures is affected by repetitive aging and regeneration, which alter their mechanical and environmental performance. Understanding these changes is critical for improving the recycling and reuse of modified asphalt in pavement engineering. In this study, SBS–nano TiO_2 composite modified asphalt underwent primary aging, primary regeneration, secondary aging, and secondary regeneration. Micro-scale tests, including gel permeation chromatography (GPC) and scanning electron microscopy (SEM), were conducted to assess morphological and molecular weight changes. Macro-scale performance tests, including dynamic shear rheometer (DSR), bending beam rheometer (BBR), rutting, bending, Marshall stability, splitting strength, and dynamic modulus tests, were used to evaluate high- and low-temperature properties, moisture resistance, and fatigue resistance. The results showed that repeated aging caused SBS degradation, reducing its molecular weight, while oxidation of asphalt components increased their molecular weight. In regenerated asphalt, aged and cracked SBS chains interwove with newly added chains, whereas nano-TiO_2 remained stable throughout aging and regeneration. High-temperature performance of asphalt and mixtures was significantly enhanced after aging, but low-temperature properties and fatigue resistance deteriorated. Regeneration partially restored these properties, though not to the level of the original material. Moisture resistance remained generally stable, with freeze–thaw splitting strength ratio decreasing by 3.3%–4.1%. The dynamic modulus increased with aging but declined after regeneration, while fatigue resistance showed the opposite trend. Overall, SBS–nano TiO_2 composite modified asphalt and mixtures exhibit superior high-temperature performance compared to the original material after repeated aging and regeneration. However, their low-temperature and fatigue properties decline progressively. Regeneration mitigates but cannot fully reverse these effects. These findings provide a performance basis for the repeated recycling of composite modified asphalt and highlight the need for strategies that better restore low-temperature and fatigue performance during regeneration.

KEYWORDS

SBS and nano-TiO_2, composite modified asphalt and mixture, repetitive aging andregeneration, microscopic morphology, high and low temperature performances, dynamic modulus, fatigue resistance

1 Introduction

SBS modified asphalt and its mixtures are widely used in asphalt pavements. By incorporating polymers such as crumb rubber, SBR, polyphosphoric acid, and epoxy resin (Zhu et al., 2022; Behnood and Olek, 2017; Fan et al., 2024), as well as nanomaterials like TiO_2, ZnO, and SiO_2 (Guo et al., 2024; Han et al., 2023), or other additives such as montmorillonite and natural asphalt (Muhammed et al., 2020; Sun et al., 2024), composite modified asphalts can be prepared to further enhance specific properties of the asphalt and its mixtures.

For composite modified asphalt, current research mainly focuses on the improvement effects of modifiers on asphalt and mixture properties. Dong et al. (2025) employed Brookfield rotational viscosity tests to analyze the effects of graphene types and dosages on the viscosity–temperature characteristics of SBS modified asphalt. Cao et al. (2023) introduced nanomaterials (TiO_2/ZnO) and basalt fiber (BF) as composite modifiers for asphalt and mixtures, evaluating their effects on asphalt properties under different dosages. Yan et al. (2023) added nano-TiO_2 and graphene composite materials to asphalt and evaluated the physical properties of the modified asphalt through multiple experiments. The results showed that the addition of nano-TiO_2 and graphene could improve the high-temperature performance and aging resistance of base asphalt. Xie et al. (2020) used nano-ZnO, nano-TiO_2, and SBS as modifiers to investigate the physical property evolution of composite modified asphalt before and after UV aging, revealing its UV aging resistance mechanism. Calandra et al. (2010) investigated, from a mechanistic perspective, how compositing TiO_2 with other materials (e.g., Ag) can tune its optical properties.

These studies demonstrate the influence of different modifiers on the performance of asphalt and its mixtures, and confirm that nano-TiO_2 can further improve the high-temperature performance and UV resistance of asphalt.

In addition, studies by Jie (2021), Li et al. (2017) have shown that nano-TiO_2 can serve as a photocatalyst when incorporated into base or emulsified asphalt, promoting the decomposition of vehicle exhaust. Carneiro et al. (2013) reported that TiO_2 can enhance the skid resistance of asphalt mixture surfaces, which helps prevent accidents caused by early autumn rainfall combining with oil and other organic compounds adsorbed on the pavement. These studies indicate that nano-TiO_2 has potential applications in new construction and maintenance of conventional asphalt pavements, porous asphalt pavements, slurry seals, micro-surfacing, and fog seals to improve environmental performance.

In practical applications, the performance degradation of asphalt and mixtures after aging is a key factor affecting durability. Segundo et al. (2024) studied the properties of photocatalytic asphalt mixtures containing nano/micro TiO_2 and micro ZnO before and after short- and long-term aging. Hu et al. (2024) used molecular dynamics simulations to investigate the molecular–atomic scale interfacial interactions between HiMA and aggregate under the action of different anti-aging materials, as well as the mechanism of seawater erosion evolution. Li et al. (2024) conducted a series of experiments to evaluate the high-temperature rheological and fatigue properties of regenerated asphalt subjected to secondary aging. Considering the regeneration demand after long-term use, regeneration performance also deserves attention. However, limited research has been conducted on the aging and regeneration behavior of SBS–nano-TiO_2 composite modified asphalt.

For conventional SBS modified asphalt and its mixtures, the reaction mechanisms and performance evolution under thermal–oxidative or UV aging and regeneration are mainly characterized by SBS degradation and chain scission, along with oxidative hardening of the asphalt components. These changes enhance the high-temperature rutting resistance of asphalt and mixtures while degrading their low-temperature crack resistance and fatigue performance (Wu et al., 2023; Wang et al., 2024; Wang et al., 2020). These performance indices can be partially restored after regeneration. Under repeated aging and regeneration, the performance evolution of SBS modified asphalt and mixtures is generally consistent with that observed after the first aging and regeneration cycle. Whether in plant-mixed hot recycling or *in-situ* thermal recycling, it is necessary to add new modified asphalt during the regeneration process to compensate for the degraded SBS and reconstruct its entangled network structure, thereby partially recovering the viscoelastic properties diminished during aging (Zhang et al., 2023; Pu, 2024; Zou et al., 2019).

In this study, micro-scale tests including gel permeation chromatography (GPC) and scanning electron microscopy (SEM), as well as macro-scale tests such as the three conventional asphalt indexes, dynamic shear rheometer (DSR), bending beam rheometer (BBR), rutting, bending, Marshall stability, splitting strength, and dynamic modulus tests were conducted. These tests cover the morphology and molecular weight of asphalt components, high- and low-temperature performance of asphalt and mixtures, moisture stability, dynamic modulus, and fatigue resistance of mixtures. The aim is to investigate the performance evolution of SBS–nano-TiO_2 composite modified asphalt and mixtures after primary aging, primary regeneration, secondary aging, and secondary regeneration.

2 Materials and methods

2.1 Preparation of various asphalt samples

A commercial SBS (I-D) modified asphalt and rutile-type nano-TiO_2 were selected. The nano-TiO_2 was incorporated at a dosage of 1% by weight of the SBS modified asphalt. The composite modified asphalt was prepared by shearing the mixture at 800 r/min for 30 min at 150 °C, as shown in Figure 1. According to the specifications in the Test Methods of Asphalt and Asphalt Mixtures for Highway Engineering (JTG E20, 2011), the original asphalt underwent short-term thermal-oxidative aging using the thin film oven test (TFOT, T0609), followed by long-term aging using the pressure aging vessel (PAV, T0630), to produce the primary aged asphalt samples.

Asphalt mixture rejuvenators are usually classified by their mechanism into rejuvenating and fluxing effects (Loise et al., 2021). A commercial rejuvenator was selected, meeting the RA5 grade requirements specified in the Technical Specification for Asphalt Pavement Recycling (JTG/T 5521, 2019); its performance indices are presented in Table 1. The rejuvenator was added to the primary aged asphalt at 150 °C at a dosage of 5% by weight of the aged asphalt, and the mixture was stirred at 300 r/min for 6 min. Since new asphalt is

FIGURE 1
Shearing process of modified asphalt.

typically added during plant-mixed or *in-situ* hot recycling of asphalt pavements, an equal amount of SBS (I-D) modified asphalt without nano-TiO_2 was added to the aged asphalt to simulate this process. The mixture was then stirred at 500 r/min for an additional 10 min to obtain the primary regenerated asphalt, as illustrated in Figure 2.

The primary regenerated asphalt was subjected to short-term and long-term aging once again to obtain the secondary aged asphalt samples. The secondary regenerated asphalt was prepared following the same regeneration procedure as that used for the primary aged asphalt.

2.2 Preparation of asphalt mixture samples

Using the previously prepared asphalt samples—original asphalt, primary aged asphalt, primary regenerated asphalt, secondary aged asphalt, and secondary regenerated asphalt—AC-13 asphalt mixtures were produced (Figure 3) shows some samples of asphalt mixture prepared from original asphalt. The mix design gradation is presented in Figure 4, which also indicates the upper and lower gradation limits for AC-13 asphalt mixtures as specified in the Technical Specifications for Construction of Highway Asphalt Pavements (JTG F40, 2004). Basalt was used as the coarse aggregate, and limestone was used for both the fine aggregate and mineral filler. The asphalt–aggregate ratio was uniformly set at 4.9%.

2.3 Test methods

In accordance with the Test Methods of Asphalt and Asphalt Mixtures for Highway Engineering (JTG E20-2011), various macro-scale performance tests were conducted on the original, aged, and regenerated asphalt and asphalt mixtures. In addition, Gel Permeation Chromatography (GPC) and Scanning Electron Microscopy (SEM) tests were performed to analyze the molecular weight distribution and microscopic morphology of asphalt samples, respectively.

For the SEM test, an FEI Inspect F50 scanning electron microscope was used to observe the microstructural characteristics of asphalt samples. In the GPC test, an Agilent 1260 Infinity high-performance liquid chromatography system was employed. Tetrahydrofuran (THF) was used as the mobile phase at a flow rate of 1 mL/min. The injection volume was 100 μL, with a sample concentration of 5 mg/mL. GPC analysis was performed on five types of asphalt samples: original, aged, and regenerated.

Under the elution effect of the mobile phase, SBS macromolecules in the composite modified asphalt exhibit shorter retention times in the gel columns compared to asphalt molecules. Therefore, based on the differences in elution peak times on the chromatogram, the SBS phase and asphalt phase can be distinguished. For each identified elution peak, the corresponding molecular phase was selected, and the number-average molecular weight (Mn), weight-average molecular weight (Mw), and polydispersity index (PDI) were calculated using Equations 1–3 to characterize the molecular weight distribution of the original, aged, and regenerated asphalt. In the equations, w_i represents the number of molecules with molecular weight M_i, w is the total number of molecules, n_i is the molar amount of molecules with molecular weight M_i, and n is the total molar amount of all molecular types (Qin et al., 2021; Ding et al. 2023).

$$M_W = \sum_{i=1}^{n} \frac{w_i \times M_i}{w} \tag{1}$$

$$M_n = \sum_{i=1}^{n} \frac{n_i \times M_i}{n} \tag{2}$$

$$PDI = \frac{M_W}{M_n} \tag{3}$$

3 Performance of asphalt under repetitive aging and regeneration

3.1 Molecular weight and microscopic morphology

The elution curves obtained from the Gel Permeation Chromatography (GPC) tests for the original asphalt, primary aged

TABLE 1 Performance indicators of the selected regenerant and nano-TiO_2.

Index	60 °C Dynamic viscosity (mPa·s)	15 °C Density (g/cm^3)	Saturate content (%)	Aromatic content (%)	Apparent Density (g/cm^3)	Specific surface area (cm^2/g)	pH value
Regenerant	707	0.991	20.9	49.8	—	—	—
RA5 Requirement	176–900	N/A	≤30	N/A	—	—	—
Nano-TiO_2	—	—	—	—	0.4	90	6–7

FIGURE 2
Preparation setup for regenerated asphalt.

FIGURE 3
Asphalt mixture specimens.

asphalt, primary regenerated asphalt, secondary aged asphalt, and secondary regenerated asphalt samples are shown in Figure 5. The number-average molecular weight (Mn), weight-average molecular weight (Mw), and polydispersity index (PDI) for both the asphalt phase and the SBS phase of the five asphalt types are presented in Figures 6, 7.

It can be observed that all elution curves of the original, aged, and regenerated SBS modified asphalt samples exhibit two prominent peaks. The elution peak between 14 and 18 min corresponds to the earlier eluting SBS phase, while the peak between 20 and 27 min corresponds to the later eluting asphalt phase. After aging, the peak intensity of the SBS phase significantly decreases. The number-average molecular weight (Mn) and weight-average molecular weight (Mw) of the SBS phase decrease by 48.3% and 41.6%, respectively, after primary aging, and by 36.3% and 31.5%, respectively, after secondary aging. It is evident that in both aging stages, the reduction in Mn is consistently greater than that of Mw, indicating that thermal-oxidative aging causes chain scission and oxidative degradation of the SBS polymer into smaller polymer fragments. This leads to a larger proportion of low-molecular-weight species in the SBS phase. Furthermore, the polydispersity index (PDI) of the SBS phase increases after both primary and secondary

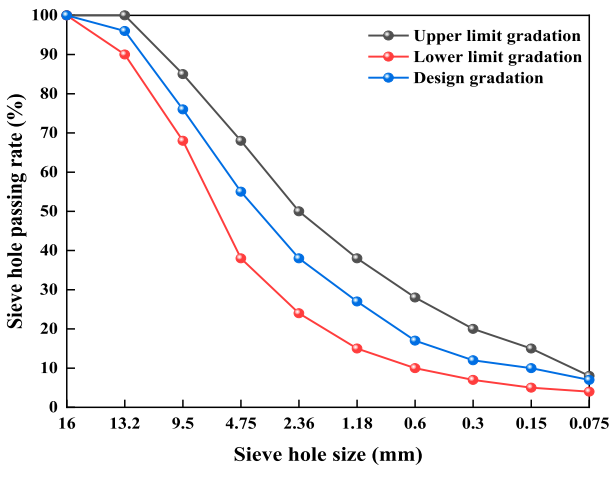

FIGURE 4
Gradation curve of AC13 asphalt mixture.

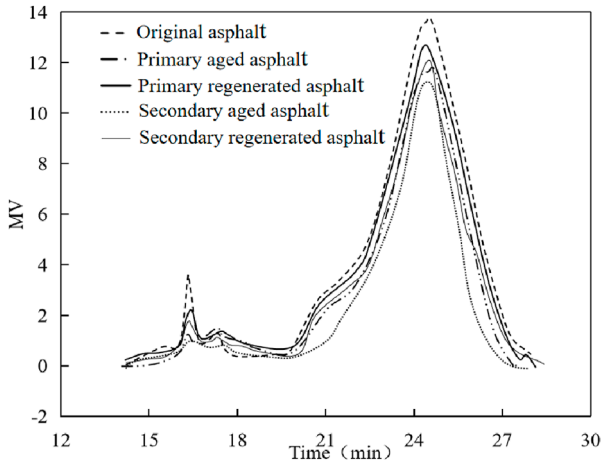

FIGURE 5
Elution curves of gel permeation chromatography tests for five asphalt samples.

aging. This is also attributed to the degradation of large molecules, which increases the disparity among molecular weights, thereby widening the gap between Mn and Mw. In contrast, the Mn and Mw of the asphalt phase both increase after primary and secondary aging, reflecting the oxidative mass gain of asphalt molecules during the aging process.

After primary or secondary regeneration, the introduction of the rejuvenator brings a significant number of small molecules into the asphalt phase, leading to a reduction in both Mn and Mw. However, these values remain higher than those of the original (unaged) asphalt, and the asphalt-phase elution peak shifts slightly to the right compared to the original asphalt. The addition of fresh SBS modified asphalt during the regeneration process introduces a large number of high-molecular-weight SBS chains, which contributes to an increase in Mn and Mw of the SBS phase by 29.7%–43.2%.

Among the five asphalt types (original, aged, and regenerated), the PDI of the asphalt phase ranges from 3.3 to 3.7, while that of the SBS phase ranges from 1.3 to 1.6. The significantly lower PDI of the SBS phase indicates that the variation in molecular weight among SBS macromolecules is relatively small. This observation is further supported by the narrower elution peak of the SBS phase compared to the much broader peak of the asphalt phase. In terms of Mn and Mw of the SBS phase, the order from highest to lowest is: original asphalt > primary regenerated asphalt > secondary regenerated asphalt > primary aged asphalt > secondary aged asphalt. For the asphalt phase, the order is: secondary aged asphalt > primary aged asphalt > secondary regenerated asphalt > primary regenerated asphalt > original asphalt.

Further SEM imaging was performed on the original asphalt, secondary aged asphalt, and secondary regenerated asphalt samples, as shown in Figure 8. In the original asphalt, the SBS chains form an interwoven network structure, and the polymer chains appear intact with smooth surfaces. In contrast, the SBS chains in the secondary aged asphalt exhibit a large number of surface cracks, indicating that molecular degradation of SBS due to aging also weakens its network structure. In the secondary regenerated asphalt, both damaged/cracked and intact/interwoven SBS chains are observed. The intact chains originate from the addition of fresh SBS modified asphalt during repeated regeneration. As an inorganic material, nano-TiO_2 remains essentially unchanged during both aging and regeneration processes.

3.2 Conventional physical properties

The conventional physical properties (penetration, softening point, and ductility) of the five asphalt samples were tested, and the results are summarized in Table 2. It can be observed that after both primary and secondary aging, the penetration and ductility values of the asphalt significantly decrease, while the softening point slightly increases. The magnitude of changes after secondary aging is greater than after primary aging. After regeneration, due to the introduction of the rejuvenator and fresh SBS modified asphalt, the lost light components (from asphalt oxidation and volatilization) and degraded SBS macromolecules are replenished (Zhao et al., 2016; Shafabakhsh et al. 2015). As a result, the penetration, ductility, and softening point of the regenerated asphalt are partially restored.

3.3 High-temperature performance

The Dynamic Shear Rheometer (DSR) test, as shown in Figure 9, was conducted using a Smart Pave 102 dynamic shear rheometer at four different temperatures: 58 °C, 64 °C, 70 °C, and 76 °C. The complex modulus G and phase angle δ of the five asphalt samples were measured, and the rutting factor $G/\sin\delta$ was calculated. The results are shown in Figures 10–12.

Among the five asphalt types, at all test temperatures, the original asphalt exhibits the lowest complex modulus and rutting factor and the highest phase angle. This is followed by the primary regenerated asphalt, then the secondary regenerated asphalt and the primary aged asphalt, while the secondary aged asphalt exhibits the highest complex modulus and rutting factor and the lowest phase angle. The relative values of complex modulus, phase angle, and rutting factor between secondary regenerated asphalt and primary aged asphalt vary with temperature.

These results indicate that both primary and secondary aging cause asphalt hardening, leading to an increase in complex modulus. The increase in elasticity of the asphalt phase due to aging outweighs the reduction in elasticity caused by partial degradation of the SBS network, resulting in a decrease in phase angle. A higher rutting factor reflects better high-temperature performance. The increase in rutting factor after aging confirms the enhancement of asphalt's high-temperature performance. At 58 °C–76 °C, the rutting factor of secondary aged asphalt is 29%–46% higher than that of the primary aged asphalt.

As the number of regeneration cycles increases, even though rejuvenator and fresh modified asphalt are added to the aged asphalt, the rutting factor of primary regenerated asphalt increases by 35%–110%, and that of secondary regenerated asphalt increases by 46%–130%, compared to the original asphalt at various

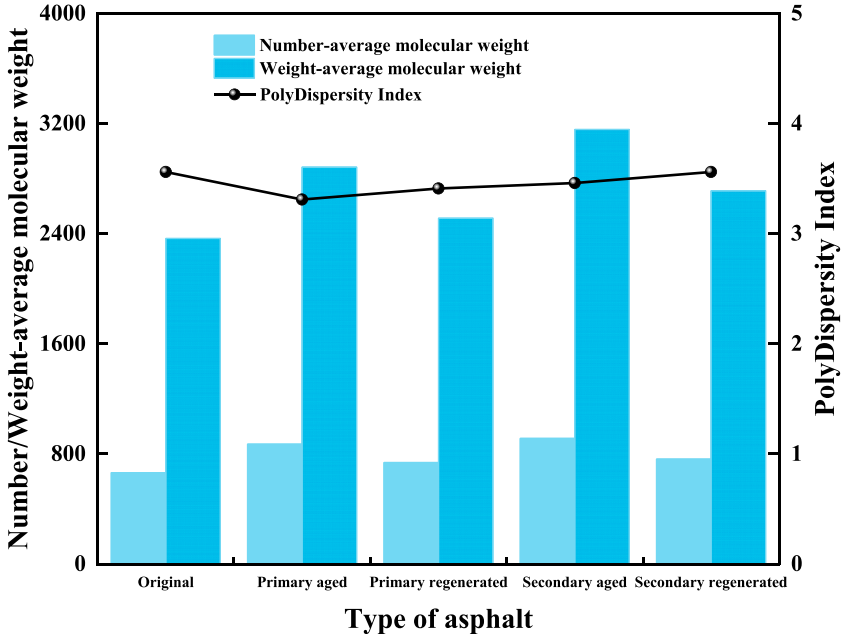

FIGURE 6
Molecular weights and dispersity indices of asphalt phases in five asphalt samples.

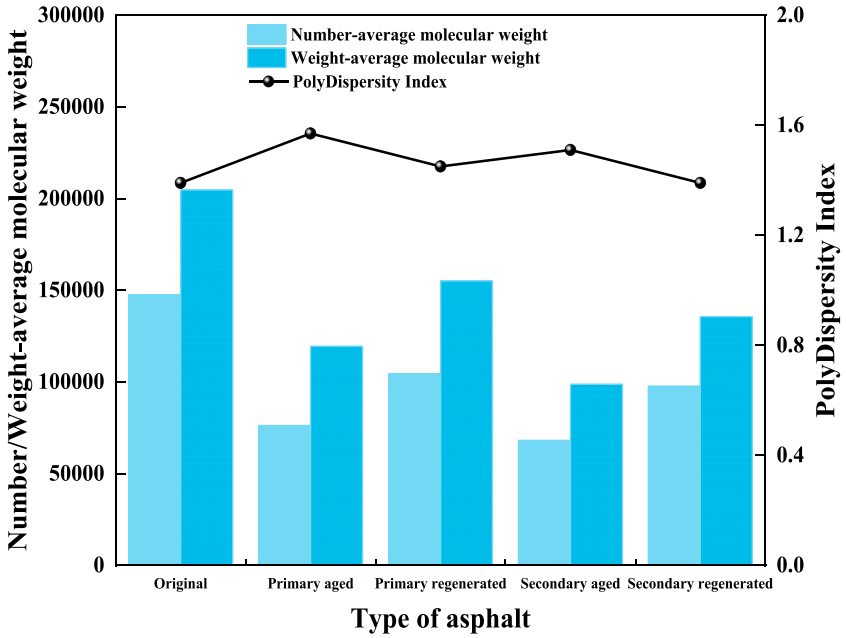

FIGURE 7
Molecular weights and dispersity indices of SBS phases in five asphalt samples.

temperatures. This indicates that, although SBS degradation occurs during aging, aging of the asphalt phase is more dominant, and the high-temperature performance of the secondary regenerated asphalt remains better than that of the original asphalt. Studies have shown that the addition of nano-TiO_2 improves the high-temperature performance of asphalt but adversely affects its low-temperature performance (Han et al., 2023; Cao et al. 2023; Zhang et al., 2023). Given that aging enhances high-temperature performance while significantly deteriorating low-temperature performance, regeneration should focus on restoring low-temperature properties. Therefore, in this study, SBS modified asphalt and rejuvenator were used to supplement the degraded SBS component and light fractions

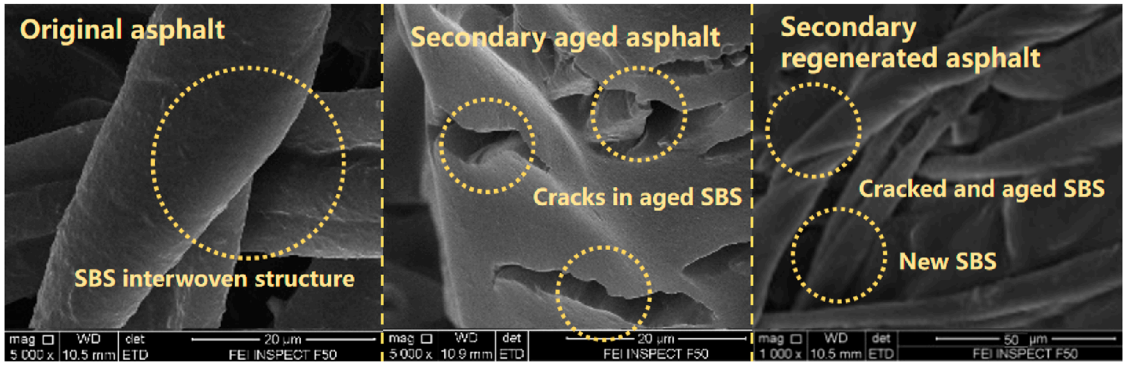

FIGURE 8
SEM images of five asphalt samples.

TABLE 2 Three major index data of five asphalt samples.

Index	Original	Primary aged	Primary regenerated	Secondary aged	Secondary regenerated
Penetration (0.1 mm)	53.8	15.4	46.2	10.4	37.1
Softening Point (℃)	81.3	84.6	76.9	83.8	78.5
Ductility at 5 ℃ (cm)	43.0	2.5	20.8	0.9	16.5

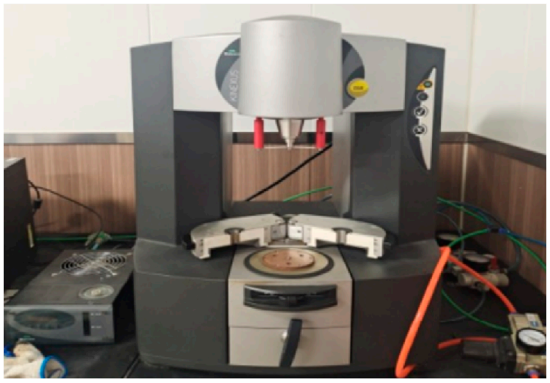

FIGURE 9
Dynamic shear rheometer (DSR) test.

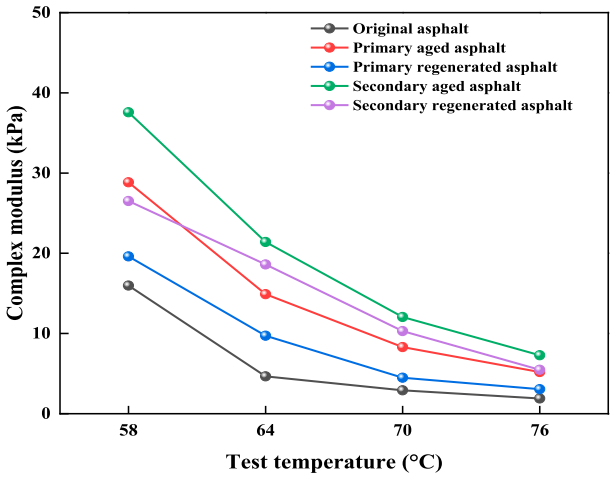

FIGURE 10
Complex moduli of five asphalt samples.

lost during aging. The use of SBS–nano-TiO_2 composite modified asphalt in regeneration is not recommended, in order to avoid further degradation of low-temperature performance.

3.4 Low-temperature performance

Tables The Bending Beam Rheometer (BBR) test was performed using a PAVETEST B216 device at three temperatures: 24 °C, −18 °C, and −12 °C, as shown in Figure 13. The creep stiffness and creep rate of the five asphalt samples were measured, and the results are shown in Figures 14, 15.

Lower creep stiffness and higher creep rate indicate better low-temperature performance of asphalt. Within the temperature range of −24 °C to −12 °C, the order of creep stiffness from largest to smallest or creep rate from smallest to largest for the five asphalt samples is: secondary aged asphalt, primary aged asphalt, secondary regenerated asphalt, primary regenerated asphalt, and original asphalt. This shows that the low-temperature performance of these five types of asphalt increases in the stated sequence. The reason is that under repeated aging, the light components

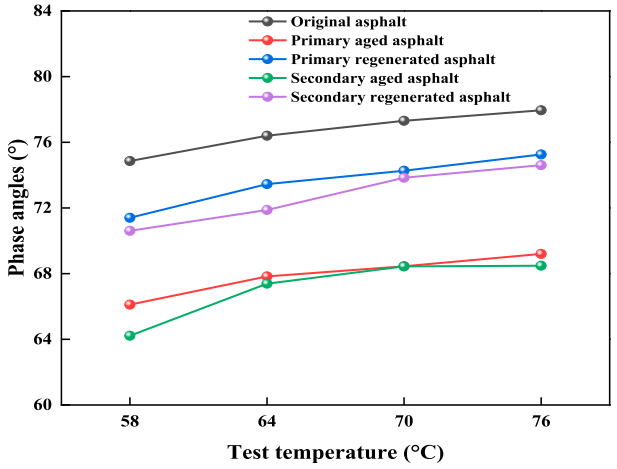

FIGURE 11
Phase angles of five asphalt samples.

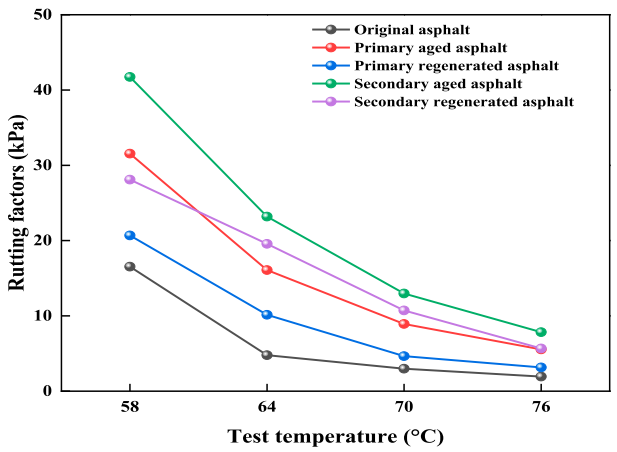

FIGURE 12
Rutting factors of five asphalt samples.

FIGURE 13
Bending beam rheometer (BBR) test.

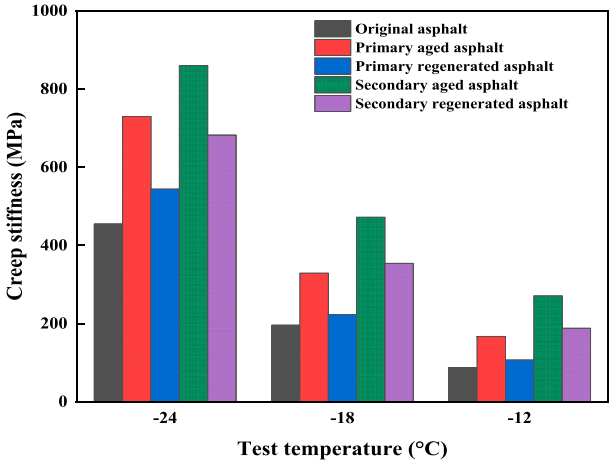

FIGURE 14
Creep stiffness of five asphalt samples.

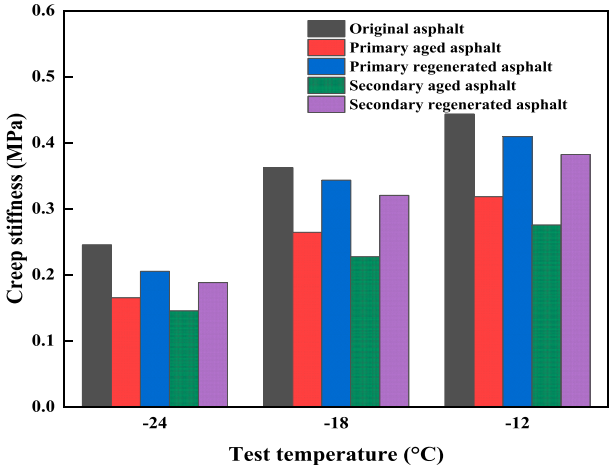

FIGURE 15
Creep rates of five asphalt samples.

FIGURE 16
Rutting test.

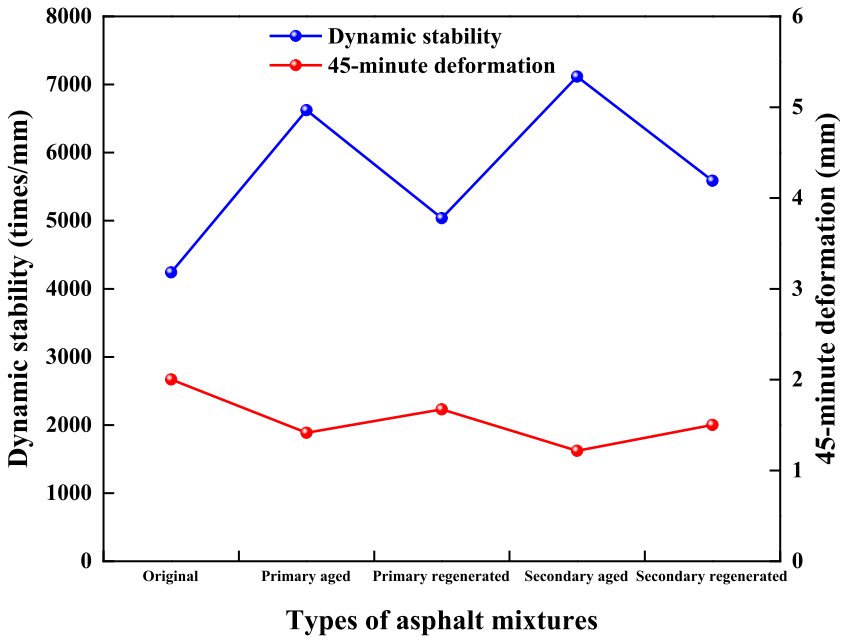

FIGURE 17
45-min deformation and dynamic stability of five asphalt mixture samples.

FIGURE 18
Bending test.

in the asphalt phase evaporate, asphalt molecules oxidize and become harder and more brittle, while macromolecules in the SBS phase degrade, and the crosslinked structure is partially destroyed. Compared with the original asphalt, at different temperatures, the creep stiffness of primary and secondary regenerated asphalt increases by 13%–23% and 50%–116%, respectively, while the creep rate decreases by 7%–20% and 13%–28%, respectively. Therefore, the low-temperature performance of asphalt after primary and secondary regeneration remains significantly lower than that of the original asphalt.

4 Performance of repetitive aging and regeneration mixtures

4.1 High- and low-temperature performance

Rutting tests were conducted at 60 °C, as shown in Figure 16. The 45-min deformation and dynamic stability of asphalt mixtures prepared with original, primary aged, primary regenerated, secondary aged, and secondary regenerated asphalt were tested to characterize their high-temperature rutting resistance. The results are presented in Figure 17. Compared with the original asphalt mixture, the 45-min deformation of the secondary regenerated asphalt mixture was still 24.0% lower, while its dynamic stability was 32.8% higher, indicating that repeated aging significantly improved the high-temperature rutting resistance of the mixture.

4.2 Low-temperature performance

Bending tests at 0 °C, as shown in Figure 18 were performed to measure bending stiffness modulus and maximum tensile strain of the five asphalt mixtures, as shown on Figure 19. A larger maximum tensile strain indicates better low-temperature crack resistance. After repetitive aging, the bending stiffness modulus of the mixtures increases, and the maximum tensile strain significantly decreases, indicating that aging greatly reduces the low-temperature performance of the composite modified asphalt mixtures. The maximum tensile strain after primary and secondary aging decreases by 52.5% and 73.4%, respectively, compared with the original asphalt.

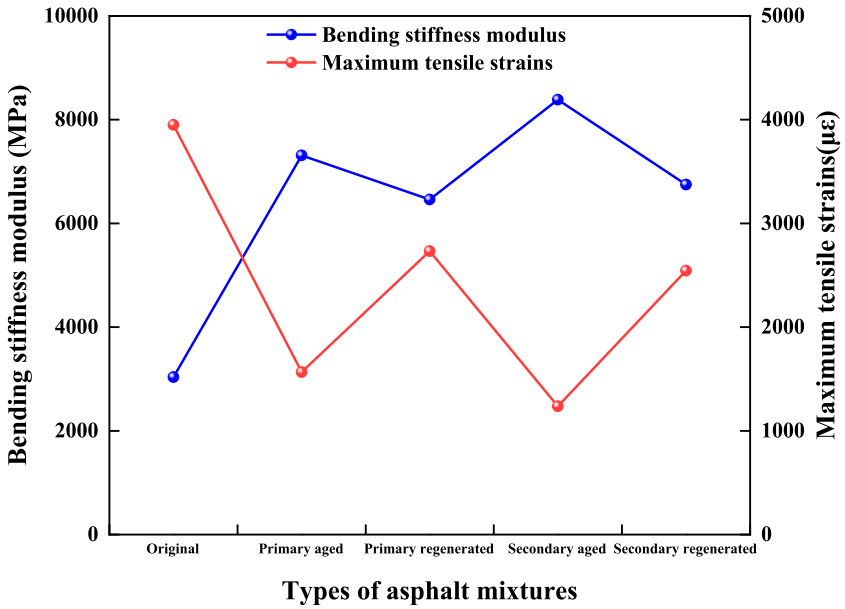

FIGURE 19
Bending stiffness modulus and maximum flexural tensile strain of five asphalt mixture samples.

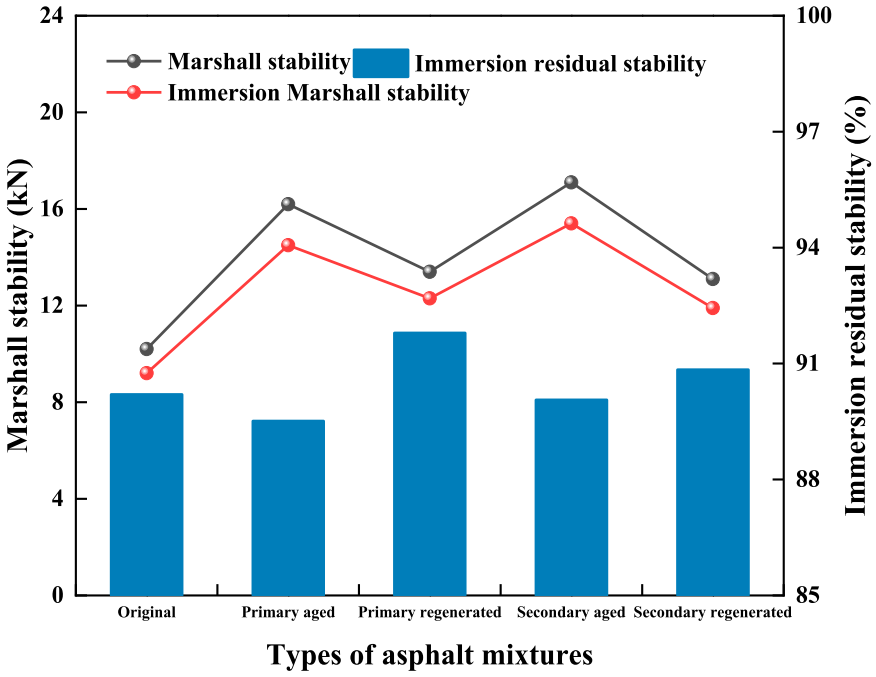

FIGURE 20
Marshall stability and immersion residual stability of five asphalt mixture samples before and after immersion.

After primary and secondary regeneration, the maximum tensile strains are 2734 με and 2512 με, slightly above the lower limit of 2500 με for modified asphalt in cold regions specified in the "Technical Specification for Construction of Highway Asphalt Pavements" (JTG F40, 2004), but still 30.1% and 38.6% lower than the original asphalt. This indicates that low-temperature crack resistance is a challenging property to maintain for SBS-nano TiO_2 composite modified asphalt mixtures during aging. Without supplementation of original composite modified asphalt during secondary regeneration, and only adding rejuvenator, it is difficult to restore the low-temperature crack resistance of the secondary aged asphalt mixture.

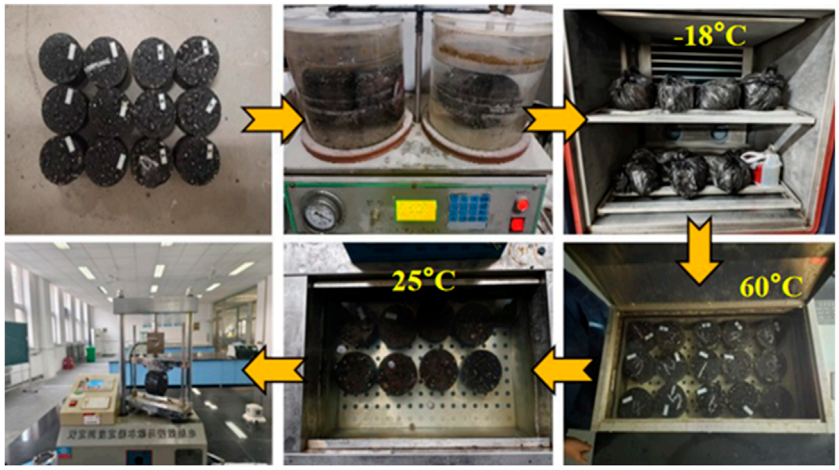

FIGURE 21
Freeze-thaw splitting test.

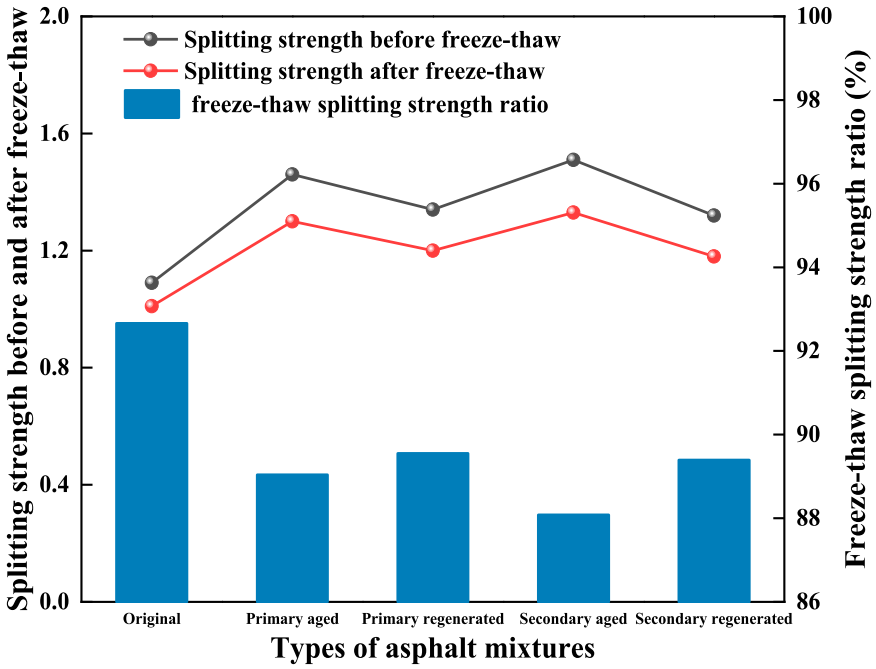

FIGURE 22
Splitting strength and freeze-thaw splitting strength ratio of five asphalt mixture samples before and after freeze-thaw.

4.3 Moisture resistance

Two groups of Marshall specimens were prepared (with no fewer than four specimens in each group) and then placed in a water bath maintained at 60 °C. One group was immersed in water for 48 h, while the other was immersed for no less than 30 min. The Marshall stability of the five asphalt mixtures was determined, and the residual stability index after water immersion was calculated, as shown in Figure 20.

The entire freeze-thaw splitting test procedure is illustrated in Figure 21. First, the Marshall specimens were subjected to vacuum treatment (vacuum pressure of 97.3–98.7 kPa for 15 min). After vacuum extraction, the specimens were soaked in water for 30 min. Subsequently, the specimens were immediately placed in a low-temperature test chamber at −18 °C and stored for 16 h to simulate freeze-thaw conditions. Prior to freezing, specimens were sealed in plastic bags containing 10 mL of water. After freezing, the specimens were immediately transferred to a constant-temperature water bath at 60 °C for 24 h of curing. Finally, the first and second groups of specimens were separately soaked in a 25 °C water bath for 2 h. After cooling, splitting strength tests were performed to obtain the load values. The freeze-thaw splitting strength ratio was calculated,

FIGURE 23
Dynamic modulus test loading process.

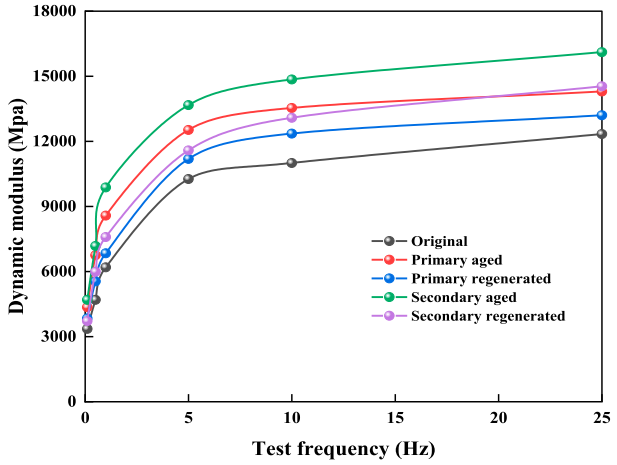

FIGURE 24
Dynamic modulus curves of five asphalt mixture samples.

FIGURE 25
Four-point bending fatigue test.

as shown in Figure 22. Higher residual stability and freeze-thaw splitting strength ratio indicate better water stability of the mixtures. Larger residual stability and freeze-thaw splitting strength ratio indicate better moisture resistance of the mixtures.

It is observed that Marshall stability before and after immersion and splitting strength before and after freeze-thaw significantly increase after aging but decrease after regeneration. This is because aging enhances the tensile and compressive properties of composite modified asphalt, but residual stability after immersion and freeze-thaw splitting strength ratio decline after aging. Aging reduces the adhesion performance at the asphalt-aggregate interface, making the interface more susceptible to various microscopic damages after water immersion or freeze-thaw cycles, leading to decreased moisture resistance of the mixtures.

After primary or secondary aging, the decrease in residual stability compared with original asphalt is within 1%, while the decrease in freeze-thaw splitting strength ratio is between 4% and 6%, but both remain above the requirements of the "Technical Specification for Construction of Highway Asphalt Pavements" (JTG F40, 2004), which requires residual stability above 85% and freeze-thaw splitting strength ratio above 80% for modified asphalt mixtures in wet regions. After primary or secondary regeneration, residual stability remains basically stable compared with original asphalt, while freeze-thaw splitting strength ratio decreases by 3.3% and 4.1%, respectively.

4.4 Dynamic modulus

According to China's "Specifications for Design of Highway Asphalt Pavements" (JTG D50–2017), the dynamic modulus at 20 °C and 5 Hz is adopted in asphalt pavement design. Therefore, for a certain degree of simplicity, the uniaxial compression dynamic modulus tests were conducted on five types of asphalt mixtures at 20 °C under six frequencies: 0.1 Hz, 0.5 Hz, 1 Hz, 5 Hz, 10 Hz, and 25 Hz. The test procedure is illustrated in Figure 23, and the resulting dynamic modulus curves are presented in Figure 24.

The dynamic modulus of the composite modified asphalt mixtures increases with frequency. At different frequencies, aging significantly increases the dynamic modulus of composite modified asphalt mixtures, indicating repetitive aging benefits the compressive performance of mixtures. Except for a few points, at the same frequency between 0 and 25 Hz at 20 °C, the order of dynamic modulus from highest to lowest is secondary aged, primary aged, secondary regenerated, primary regenerated, and original asphalt mixtures. At 20 °C and 10 Hz, dynamic modulus is a key indicator for characterizing mechanical performance of asphalt surface layers in structural design. After primary and secondary regeneration, it remains 22.0% and 33.2% higher than that of the original asphalt mixture, respectively.

4.5 Fatigue resistance

Four-point bending fatigue tests were performed at 15 °C and 10 Hz to measure the number of loading cycles corresponding to the bending stiffness modulus decreasing to 50% of its initial value,

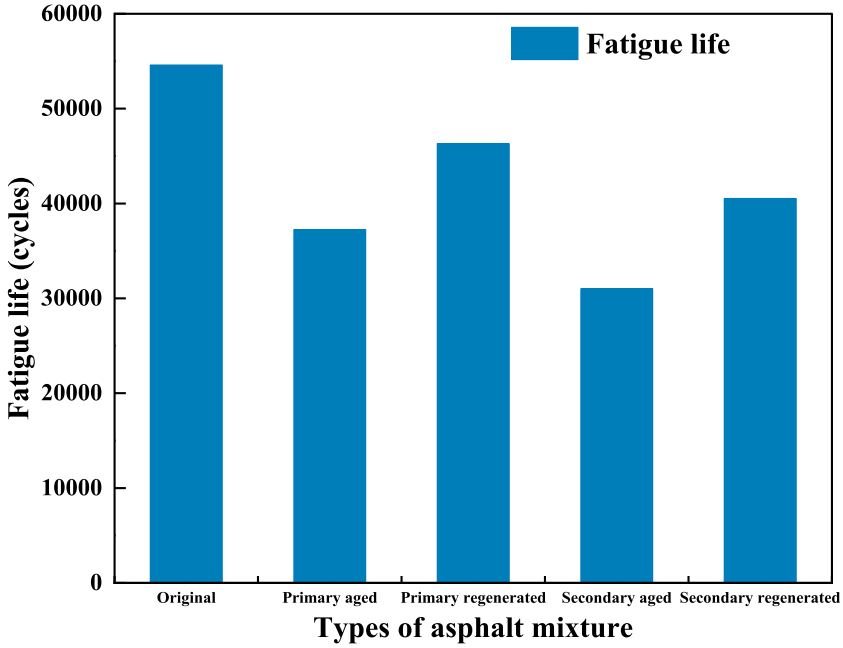

FIGURE 26
Fatigue life of five asphalt mixture samples.

defined as fatigue life. The test procedure is illustrated in Figure 25. The results are shown in Figure 26.

Fatigue life of composite modified asphalt mixtures significantly decreases with aging and partially recovers after regeneration. However, fatigue life after primary and secondary regeneration remains 15.0% and 26.2% lower than the original asphalt mixture, respectively. Although fresh modified asphalt is added during regeneration, degraded SBS chains cannot be restored, and new and old asphalt molecules cannot fully integrate, increasing internal micro-damage. Compared with the original asphalt, the asphalt-aggregate interface bonding weakens after regeneration, and numerous weak areas exist internally and at bonding interfaces under repeated loading. Thus, fatigue resistance of the five mixtures ranks from highest to lowest as: original, primary regenerated, secondary regenerated, primary aged, and secondary aged asphalt mixtures.

5 Summary and conclusion

This study systematically investigated the performance evolution of SBS–nano TiO_2 composite modified asphalt and mixtures after primary aging, primary regeneration, secondary aging, and secondary regeneration, by combining micro-scale tests such as Gel Permeation Chromatography (GPC) and Scanning Electron Microscopy (SEM) with macro-scale tests including Dynamic Shear Rheometer (DSR), Bending Beam Rheometer (BBR), rutting test, bending test, Marshall stability, and dynamic modulus. The main conclusions are as follows:

1. Repetitive aging causes degradation of the SBS phase and decreases its molecular weight, while oxidation of the asphalt phase increases its molecular weight. Regeneration can increase the molecular weight of the SBS phase by supplementing new SBS chains. The secondary regenerated asphalt contains both damaged and intact interwoven SBS chains. Nano TiO_2 remains stable in properties throughout aging and regeneration.
2. Aging significantly enhances the high-temperature performance of asphalt and mixtures but severely deteriorates low-temperature performance and fatigue resistance. After regeneration, high-temperature performance remains higher than that of the original asphalt, while low-temperature and fatigue performances show some recovery but remain significantly lower than the original state.
3. The moisture stability of mixtures slightly decreases after aging; after regeneration, residual stability after water immersion remains basically stable, and the freeze-thaw splitting strength ratio decreases slightly, but both meet specification requirements. Dynamic modulus increases with aging and decreases with regeneration, whereas fatigue resistance exhibits the opposite trend.

Based on the above findings, it can be concluded that the original and primary regenerated composite modified asphalt are suitable for conventional or medium-traffic pavements that require balanced high- and low-temperature performance and fatigue resistance. In contrast, primary aged, secondary aged, and secondary regenerated composite modified asphalt are more appropriate for high-temperature heavy-load pavements or special sections with lower low-temperature performance requirements.

Future work may involve long-term field exposure tests combined with actual environmental factors (such as ultraviolet radiation and precipitation) to further validate the evolution laws of repetitive aging and regeneration performance. Additionally, the synergistic mechanisms of SBS–nano TiO_2 composite

modified asphalt in repetitive aging and regeneration with other nanomaterials (e.g., graphene, carbon nanotubes) warrant further investigation.

Data availability statement

The original contributions presented in the study are included in the article/supplementary material, further inquiries can be directed to the corresponding author.

Author contributions

XF: Software, Conceptualization, Resources, Project administration, Methodology, Writing – original draft. GS: Validation, Data curation, Writing – review and editing, Supervision. JF: Investigation, Writing – review and editing, Funding acquisition, Visualization. FT: Writing – review and editing, Conceptualization, Writing – original draft.

Funding

The author(s) declare that financial support was received for the research and/or publication of this article. This research was funded by National Key Research and Development Project (2020YFA0714302), Jinling Institute of Technology (No. jit-b-202401), National Natural Science Foundation of China (No. 51878164), Guiding Science and Technology Research Project of Quzhou City (2024ZD164), and Xizang Autonomous Region Science and Technology Funding (No. XZ202501JX0006).

Acknowledgments

The authors would like to thank Tao Ma of Southeast University for his guidance and advice in revising this article.

Conflict of interest

The authors declare that the research was conducted in the absence of any commercial or financial relationships that could be construed as a potential conflict of interest.

Generative AI statement

The author(s) declare that no Generative AI was used in the creation of this manuscript.

Any alternative text (alt text) provided alongside figures in this article has been generated by Frontiers with the support of artificial intelligence and reasonable efforts have been made to ensure accuracy, including review by the authors wherever possible. If you identify any issues, please contact us.

Publisher's note

All claims expressed in this article are solely those of the authors and do not necessarily represent those of their affiliated organizations, or those of the publisher, the editors and the reviewers. Any product that may be evaluated in this article, or claim that may be made by its manufacturer, is not guaranteed or endorsed by the publisher.

References

Behnood, A., and Olek, J. (2017). Rheological properties of asphalt binders modified with styrene-butadiene-styrene (SBS), ground tire rubber (GTR), or polyphosphoric acid (PPA). *Constr. Build. Mater.* 151, 464–478. doi:10.1016/j.conbuildmat.2017.06.115

Calandra, P., Ruggirello, A., Pistone, A., and Turco, L. V. (2010). Structural and optical properties of novel surfactant coated TiO2–Ag based nanoparticles. *J. Clust. Sci.* 21 (4), 767–778. doi:10.1007/s10876-010-0330-x

Cao, X. Y., Li, W. K., Shao, J. G., Wang, M. L., and Chen, J. H. (2023). Performance study of TiO_2/ZnO-BF composite modified asphalt and mixture. *J. Highw. Transp. Res. Dev.* 40, 38–45+52.

Carneiro, J., Azevedo, S., Teixeira, V., Fernandes, F., Freitas, E., Pereira, H., et al. (2013). Development of photocatalytic asphalt mixtures by the deposition and volumetric incorporation of TiO_2 nanoparticles. *Constr. Build. Mater.* 38, 594–601. doi:10.1016/j.conbuildmat.2012.09.005

Ding, W. J., He, X. Y., Yang, Y. H., Chen, Z. W., and Wang, H. P. (2023). Study on rheological properties and mechanism of rubber asphalt based on reaction parameters. *Highway* 68, 403–409.

Dong, J., Yang, B. C., Xie, W., Liu, K., and Wang, H. P. (2025). Study on viscosity-temperature characteristics and mechanism of graphene-SBS composite modified asphalt. *J. Wuhan. Univ. Technol. Transp. Sci. Eng.* 49, 102–107+112.

Fan, Y., Zhou, Y., Chen, B., Li, W., Wang, H., Wu, Y., et al. (2024). Material design and mechanism explanation of epoxy asphalt toughened with SBS/CR and CSR. *J. Mater. Civ. Eng.* 36, 04024215. doi:10.1061/JMCEE7.MTENG-17958

Gomes, D., Lages, D., Pereira, F., Costa, L., Gomes, J. R. B., and Figueiredo, F. (2019). Photocatalytic asphalt pavement: the physicochemical and rheological impact of TiO_2 nano/microparticles and ZnO microparticles onto the bitumen. *Road. Mater. Pavement Des.* 20, 1452–1467. doi:10.1080/14680629.2018.1453371

Guo, Y. R., He, Z. H., Tan, L., Wang, X. M., and Li, H. Y. (2024). Performance study of nano-SiO_2/SBS modified asphalt mixture. *Pet. Asph.* 38, 40–43+59.

Han, D., Hu, G., and Zhang, J. (2023). Study on anti-aging performance enhancement of polymer modified asphalt with high linear SBS content. *Polymers* 15, 256. doi:10.3390/polym15020256

Hu, M., Zhou, C., Sun, G., Gu, X., Polaczyk, P., Zhang, Y., et al. (2024). Molecular-atomic scale insight on asphalt–aggregate interface interaction and seawater erosion with different aging-resistant materials using molecular dynamics simulations. *Energy fuels.* 38, 9438–9457. doi:10.1021/acs.energyfuels.4c00938

Jie, Y. D. (2021). *Experimental study on photocatalytic glass microsurfacing mixture for degrading vehicle exhaust*. Yangzhou, China: Yangzhou University. Master's Thesis.

JTG E20 (2011). *Standard Test methods of asphalt and asphalt mixtures for highway engineering*. Beijing, China: China Communications Press. [In Chinese].

JTG F40 (2004). *Technical specifications for construction of highway asphalt pavements*. Beijing, China: China Communications Press.

JTG/T 5521 (2019). *Technical specification for asphalt pavement recycling*. Beijing, China: China Communications Press.

Li, W. J. (2021). *Research on the performance of nano-titanium dioxide photocatalytic pervious concrete for degrading vehicle exhaust*. Changchun, China: Jilin University. Master's Thesis.

Li, W. B., Yu, J., and Li, L. P. (2017). Research on nano-TiO_2 seal coat photocatalytic decomposition exhaust asphalt pavement. *China Foreign Highw.* 37, 36–40. [In Chinese].

Li, B., Guan, Y., Zhang, Y., Wang, H., and Ma, T. (2024). Experimental study on high-temperature rheological and fatigue performance of secondary aged recycled asphalt. *Highway* 69, 366–372. [In Chinese].

Loise, V., Calandra, P., Abe, A. A., Porto, M., Rossi, C. O., Davoli, M., et al. (2021). Additives on aged bitumens: what probe to distinguish between rejuvenating and fluxing effects? *J. Mol. Liq.* 339, 116742. doi:10.1016/j.molliq.2021.116742

Muhammed, E., Erkut, Y., Vural, K., Cahit, T., Norambuena-Contreras, J., Garcia, A., et al. (2020). Effects of different bitumen modifiers on the rutting and cracking resistance of hot mix asphalts. *Int. J. Pavement Eng.* 21, 703–712. doi:10.1080/10298436.2018.1506122

Pu, J. C. (2024). *Performance Study and carbon emission quantitative calculation of secondary In-Situ hot recycled asphalt mixture. Master's thesis*. Yangzhou, China: Yangzhou University. [In Chinese].

Qin, Y., Meng, Y., Lei, J., Zhang, W., Kong, L., Yang, X., et al. (2021). Study on the microscopic characteristics and rheological properties of thermal-oxidative aged and virgin-old recycled asphalts. *Eur. Polym. J.* 154, 110499. doi:10.1016/j.eurpolymj.2021.110499

Segundo, I. R., Ferreira, C., Freitas, E. F., Carneiro, J. O., Fernandes, F., Júnior, S. L., et al. (2018). Assessment of photocatalytic, superhydrophobic and self-cleaning properties on hot mix. *Constr. Build. Mater.*166, 500–509. doi:10.1016/j.conbuildmat.2018.01.106

Shafabakhsh, G. H., Faramarzi, M., and Sadeghnejad, M. (2015). Use of surface free energy method to evaluate the moisture susceptibility of sulfur extended asphalts modified with antistripping agents. *Constr. Build. Mater.*98, 456–464. doi:10.1016/j.fuel.2016.07.018

Sun, J. S., Pu, X. T., Yang, K., Li, M. H., and Zhang, F. W. (2024). Determination of optimal dosage and performance evaluation of montmorillonite/SBS/HVA high viscosity modified asphalt modified by silane coupling agent. *China Plast.* 38, 18–25. [In Chinese].

Wang, J., Qin, Y., Xu, J., Xiao, F., Wang, F., Wang, W., et al. (2020). Crack resistance investigation of mixtures with reclaimed SBS modified asphalt pavement using the SCB and DSCT tests. *Constr. Build. Mater.* 265, 120365. doi:10.1016/j.conbuildmat.2020.120365

Wang, W., Sun, L., Li, M., Guo, H., Ma, F., Sun, Y., et al. (2024). Mechanical properties and micro mechanisms of SBS-modified asphalt binder under multiple aging and regeneration effects. *J. Mater. Civ. Eng.* 36, 04024284. doi:10.1061/JMCEE7.MTENG-17561

Wu, T. R., Li, H., Xu, J. H., Chen, Z. H., and Liu, P. (2023). Discrete element analysis of composite skeleton and mesomechanical properties of recycled asphalt mixture. *J. Wuhan. Univ. Technol. Transp. Sci. Eng.* 47, 1152–1158.

Xie, X. B., Ma, P., Liang, L. Y., Zhang, C. L., and Huang, W. D. (2020). Evaluation of UV aging resistance performance of nano-TiO_2 synergistically nano-ZnO/SBS composite modified asphalt. *Bull. Chin. Ceram. Soc.* 39, 2354–2361. [In Chinese].

Yan, K., Shi, K., Wang, M., You, L., and Wang, D. (2023). Performance of Nano-TiO_2/Graphene composite modified asphalt. *J. Mater. Civ. Eng.* 35, 04023393. doi:10.1061/JMCEE7.MTENG-15897

Zhang, W. W., Wang, X. Y., Liu, K., Li, J. W., and Chen, H. X. (2023). Evaluation of rheological properties of mineral oil regenerated asphalt after secondary aging. *J. Wuhan. Univ. Technol. Transp. Sci. Eng.* 47, 545–550.

Zhao, X., Wang, S., Wang, Q., and Yao, H. (2016). Rheological and structural evolution of SBS modified asphalts under natural weathering. *Fuel*184, 242–247. doi:10.1016/j.fuel.2016.07.018

Zhu, Y., Xu, G., Ma, T., Huang, W., and Ma, F. (2022). Compounding optimization of SBS-SBR high-viscosity modifier and rejuvenation of aged SBS-SBR modified asphalt. *J. Test. Eval.* 50, 2507–2528. doi:10.1520/JTE20220035

Zou, G. L., Qin, H., Yan, R., Liu, K., Li, J., and Zhang, H. (2019). Evaluation of multiple regeneration effects of SBS modified asphalt based on viscoelastic properties. *J. South China Univ. Technol. Nat. Sci. Ed.* 47, 75–82.